Abstract

MCCRAW, JENNIFER LEIGH. Observations on Upstream Flame Propagation in Ignited Hydrocarbon Jets. (Under the direction of Dr. Kevin Lyons.)

Studies are presented that examine the development of combustion in an initially non-reacting methane jet after ignition at a downstream location. Image measurements depicting the axial location of a fixed energy ignition source that permits transient flame propagation back to the nozzle are presented. The results from the experimental investigations are discussed. Nine different cases were investigated in order to determine the major parameters that impact the axial location of the ignition source at which flame propagation back to the burner was permitted. When the ignition source was located at larger axial distances than those indicated, flame propagation upstream to the burner was not possible and, instead, the flame blew out. The Reynolds number of the jet, the scalar field and the air co-flow magnitude were investigated for their contributions. A standard digital video camera was used in order to film the ignition of the jet and to determine the farthest axial location from the burner at which upstream flame propagation was possible. With the aid of computer software, the height for each case was determined. Conclusions to the effect these parameters had on the axial location are discussed as well as the implications for the physics governing the process.

Observations on Upstream Flame Propagation in Ignited Hydrocarbon Jets

by

Jennifer McCraw

A thesis submitted to the Graduate Faculty of
North Carolina State University
In partial fulfillment of the
Requirements for the degree of
Master of Science

Mechanical Engineering

Raleigh, NC

2006

Approved by:

_____
Dr. Kevin Lyons
(Chair of Graduate Advisory Committee)

_____ _____
Dr. Eric Klang
(Advisory Committee Member)

Dr. James Leach
(Advisory Committee Member)

Dedication

To my mom and dad:

This could not have been possible
without all your love and support throughout the years.
Thanks!

And

To my grandparents:

For all the love they showed when I was a child
I miss ya'll!

Biography

I, Jennifer Leigh McCraw, a lifelong resident of Durham, North Carolina was born November 6, 1981 to Roger and Phyllis McCraw. I grew up in Durham with my parents and older brother, but spent most summers and breaks from school in Cana, Virginia with my grandparents. I graduated from Riverside High School in 2000. Upon graduation, I was not sure whether or not to attend college, so I enrolled at Durham Technical Community College in order to give it a try. After completing one year at Durham Tech, I enrolled at North Carolina State University in 2001. All my life, I always had to take everything apart to see how it worked. Because of this, I thought Mechanical Engineering might be a good major. I graduated in May 2004 with a Bachelor of Science in Mechanical Engineering. I began graduate school in August 2004 and began my studies in experimental combustion.

Acknowledgments

I would like to thank my advisor, Dr. Lyons, for the “hands off” approach which allowed me to do my own thing, and for all the support and guidance.

Thanks to my graduate committee, Dr. Klang and Dr. Leach, for allowing me to do a project which interested me.

I would like to acknowledge Nancy Moore for all the help and guidance she gave as well as all the good times at the lab.

I would also like to thank all the friends I have made while working in the undergraduate labs, Dale Myatt, Dr. Chau Tran, David Webber, Sheldon Sigmon, and Sarah Fisher, for all their encouragement and support.

Table of Contents

List of Figures

List of Tables

1. Introduction

In regards to combustion, there are two extreme types of combustion: premixed and non-premixed. Premixed combustion occurs when the fuel and oxidizer are completely mixed before they enter the combustion chamber. Non-premixed combustion occurs when the fuel and oxidizer enter the combustion chamber separately. As with anything, there are advantages and disadvantages to each extreme. The ideal situation is to have a scenario where the advantages of each are utilized. Such a situation has been termed partially premixed combustion. Partially premixed combustion occurs when the fuel and oxidizer enter the combustion chamber separately as in non-premixed combustion but due to turbulence become partially mixed before combustion takes place.

At low jet velocities, a turbulent flame will be attached to the nozzle. In order to achieve a lifted turbulent flame, the jet velocity must be increased. This increase in velocity causes the flame to stretch and eventually the flame becomes disrupted. As a result, the flame lifts off the nozzle and stabilizes at a point downstream. The velocity at which this occurs is called the lift-off velocity. The distance between the burner and the base of the lifted flame is called the lift-off height.

If the jet velocity is decreased after lift-off is achieved, the turbulent flame will reattach to the nozzle. However, the velocity at which it reattaches is not the same as the velocity at which it lifts-off. This difference causes a hysteresis phenomenon between lift-off and reattachment. As the jet velocity is increased, the lift-off height also increases until a critical height is reached. Once this critical height is reached, if the jet velocity is increased anymore the flame will completely blow-off.

1.1 Purpose

While laminar lifted jet flames have been extensively investigated both analytically and experimentally, transitional and turbulent regions have received less attention [1]. The goal of this study is to investigate downstream ignition in initially non-reacting turbulent hydrocarbon jets issuing with air co-flow [2]. The farthest distance from the burner at which the flame will propagate upstream to its stable position upon application of an ignition source, hereafter referred to as the "upper propagation limit", is determined and presented for eleven different cases. The eleven prime cases consist of three jet Reynolds numbers at three co-flow velocities with the addition of two outlier cases. The purpose of performing these particular experiments is to gain a better understanding of the mechanism which causes a hydrocarbon flame to propagate upstream and stabilize at some point downstream from the burner nozzle. It is known that the flame will propagate however, what drives the propagation is still unknown. Many theories exist as to what the driving force is but none fully explain the phenomenon. Visual evidence of one of these theories is presented for the eleven cases studied.

1.2 Stabilization Theories for Lifted Flames

Over the last 50 years many different theories have emerged as to what causes a flame to stabilize at a point downstream from the nozzle. At times it seems as though many of these theories either contradict one another or overlap one another. No one theory can be accurately applied to all lifted flames. Until a theory is developed that can accurately portray all lifted flames in all regimes, research in this area will continue. The existing theories can be summarized in the following three categories:

- Premixed Theory

- Large Scale Structures, Scalar Dissipation and Flamelet Extinction
- Triple Flames

1.2.1 Premixed Theory

One of the earliest flame stabilization theories was presented by Wohl et al [3]. They proposed that when the mean velocity gradient at the burner exceeds some critical value the diffusion flame will lift-off. The lifted flame will then stabilize downstream where the turbulent burning velocity equals the mean flow velocity.

This was later extended by Vanquickenborne and van Tiggelen [4]. They proposed that fuel and air are completely premixed at the base of a lifted diffusion flame and that stabilization occurs when the turbulent burning velocity of the fuel and oxidizer is in equilibrium with the average flow velocity of the entering fluid. Thus the turbulent burning velocity counters the incoming jet velocity. This was somewhat addressed by Eickhoff et al [5]. They found regions at the base of the flame which were 40 to 50 percent fuel. This would cause the fuel and oxidizer mixture to react quickly and would allow the flame base to stabilize upstream from the incoming fuel.

Kalghatgi [6] tries to establish a relation for the turbulent burning velocity. Through his experiments many connections were made between lift-off height and experimental parameters. He proved that the lift-off height is essentially a linear function of jet exit velocity, is nearly independent of nozzle diameter, and is inversely proportional to the square of the maximum laminar burning velocity. He explained these results using the premixed model presented by Vanquickenborne and van Tiggelen.

Recently, Kalghatgi's work has been extended by Brown et al [7]. They conclude that the turbulent burning velocity is indeed a good indicator of flame stabilization position in

the far-field. However, they found that in the near-field, three times the laminar burning velocity is a better indication of the position of a stable flame.

1.2.2 Large Scale Structures, Scalar Dissipation, and Flamelet Extinction

Broadwell et al. [8] suggest that large scale turbulent structures are responsible for flame stabilization. They proposed a model where flame stabilization is due to hot reaction products being carried by large vertices to the edge of the jet where they reenter the mixture with fresh air. According to this idea flame lift-off and blow-out occur when the reentering products are mixed with unburned reactants too rapidly for a reaction to take place.

After doing experiments using Laser-Induced Fluorescence (LIF), Clemens and Paul [9] confirmed the presence of a quasi-laminar diffusion flame near the nozzle inlet. They also showed that the effect of heat release is to laminarize local turbulence. They also suggest that flame extinction occurs when large three-dimensional vertical structures appear downstream.

From a two-dimensional unsteady simulations of turbulent jet diffusion flames, Yamashita et al. [10] conclude that occasional extinction occurs when large values of local scalar dissipation rates produce a rupture of the reaction zone.

In contrast to the premixed flame theory, Peters and Williams [11], argue that there is not sufficient time for the fuel and oxidizer to mix such that a premixed flame is not possible. They suggest that stabilization is supported by the extinction of diffusion flamelets. This theory is also known as quenching of diffusion flamelets. Instead of the equilibrium of velocities in order to support flame stabilization, this theory suggests that the diffusion flame moves downstream to a point where the scalar dissipation rate is sufficiently low.

1.2.3 Triple Flames

Another theory for the mechanism of flame stabilization which is different from all other ideas is that of the triple flame. The triple flame theory was first introduced by Phillips [12]. This theory states that the base of the flame is composed of three different regions. These three regions are the outer fuel-lean premixed branch (on the oxidizer side), the inner fuel-rich premixed branch (on the unburned fuel side), and the trailing diffusion flame. The leading edge of the flame is the triple point which propagates in the vicinity of stoichiometric mixture. Both lean and rich branches propagate with a lower burning velocity. Behind the triple point a diffusion flame develops.

Liñán [13] and Veyante et al. [14] show theoretically that in laminar flow, lifted flames are stabilized by the triple flame configuration. Müller et al. [15] extend this idea to turbulent flames. They assume that the leading edge of a partially premixed turbulent flame is composed of a number of laminar triple flamelets. This model was used to explain the flame stabilization mechanism in lifted turbulent jet diffusion flames.

Muñiz and Mungal [16] used particle image velocimetry (PIV) to measure the instantaneous two-dimensional velocity fields in the region of a lifted flame base. They found that at the instantaneous leading edge of the flame front, the local axial velocity does not exceed three times the maximum laminar burning velocity. They concluded that the structure of the leading edge flame front exhibits similarities to the triple flame.

2. Upper Propagation Limit Experiments

2.1 Experimental Setup

The apparatus used in these experiments is illustrated in figure 1. It consists of a central fuel nozzle surrounded by a concentric air co-flow. This particular burner was

designed to deliver a “top hat” air velocity profile at the exit of the co-flow region near the nozzle exit. The co-flow air is delivered to the burner by a Magnetek model 9467 centrifugal blower. The co-flow air enters the burner at (A) and has to make an almost 90° turn at (B). The air must then go through a 2.54 cm thick honeycomb material, (C), which acts as a flow straightener. There is a 2.54 cm outside diameter hollow tube, (D), that goes through the center of the honeycomb. The fuel nozzle, (E), goes through this rod so that the fuel nozzle may be changed out with different diameter nozzles. After the air flows through the honeycomb material, it enters the diffuser section of the burner, (F), which has a greater cross-sectional area. Once in the diffuser section the air passes through four wire mesh screens in order to straighten the flow even more. After the air passes through the screens it enters a contraction section, (G) which causes the velocity of the air to increase further and then the air leaves the burner. The diameter of the burner exit is 150 mm. The hollow rod that the fuel tube is inserted in ends at (H) but the fuel nozzle continues to the exit of the burner. This setup allows for control of the fuel velocity as well as the co-flow velocity.

The fuel flow rate was measured using an Advance Series 150 flowmeter which measured in slpm, from which the jet exit velocity of methane was calculated.

The co-flow velocity was measured using a TSI Velocicalc model 8345 which gave a digital readout in m/s of the air co-flow to the nearest 0.01 m/s with an accuracy of ± 3% of the reading. The meter was placed perpendicular to the flow direction in the same position for each data acquisition run.

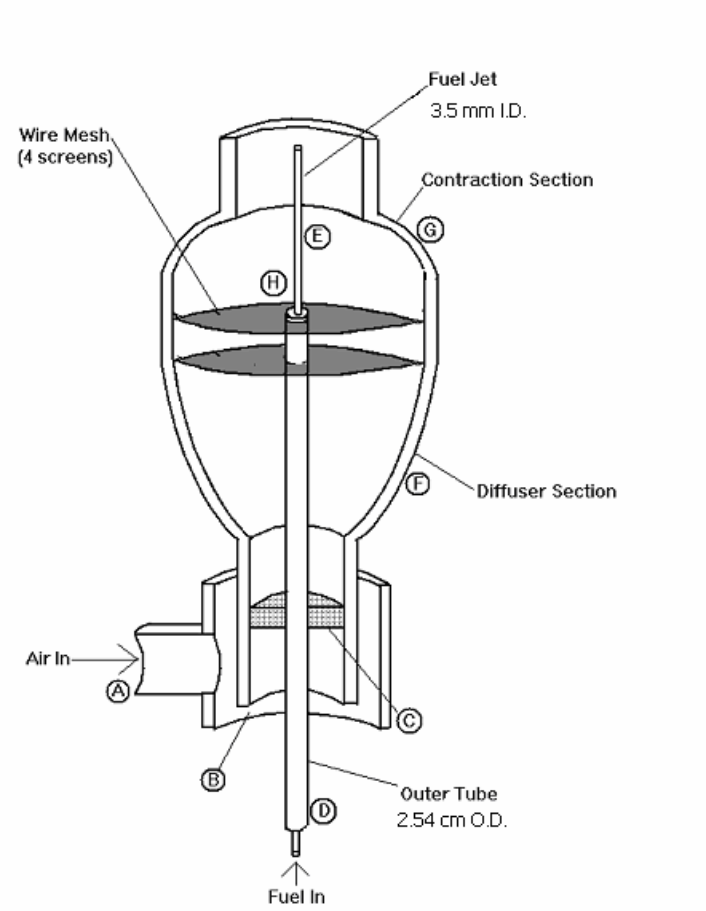

Figure 1: Schematic of the burner used for all experiments

There were nine base cases studied and two outlier cases. These nine base cases consisted of three different stable lifted heights at three co-flow velocities. The stable lift-off heights used for this study were 7.62 cm, 10.16 cm, and 13.97 cm. Each stable height was studied at each of the following co-flow velocities: 0 m/s, 0.36 m/s, and 0.49 m/s. The stable heights studied in the outlier cases were attached (not lifted) and 15.24 cm lifted above the burner. There was no co-flow velocity with either of the outlier cases. All eleven cases studied used methane as the fuel and a 3.5 mm (inside diameter) fuel nozzle.

All the images were recorded using a standard digital video camera. The camera used was a Panasonic Model PV-GS120 that produced thirty frames per second. Once the experiments were recorded the video was transferred to a computer and analyzed using Adobe Premiere Pro and Adobe Photoshop Elements. During the filming of the images, a grid of known dimension was filmed before each run in order to determine a scaling factor between the actual and Photoshop images. Once the scale factor was determined the measurements in Photoshop could be converted to actual measurements in real time.

Figure 2 shows how the experiments were conducted. The fuel and co-flow were turned on. Then the ignition source was inserted along the centerline of the fuel nozzle at a distance far enough away from the nozzle that only local burning would occur. The ignition source was then lowered (upstream) very slowly until it reached a distance close enough to the nozzle exit that flame propagation upstream was possible instead of just burning locally.

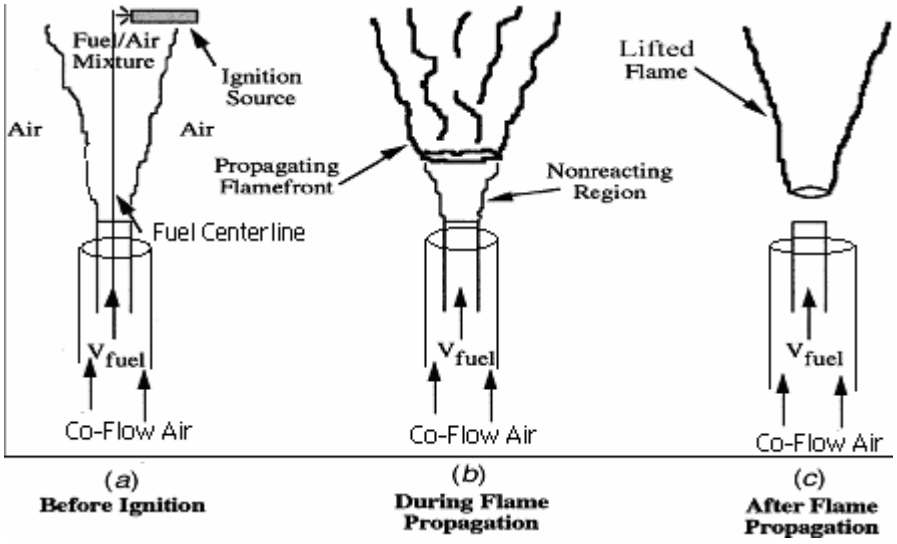

Figure 2: Approximate conduction of experiments.

a) Before ignition, b) During flame propagation, and c) After flame propagation

2.2 Upper Propagation Limit Results for Nine Base Cases

Figure 3 is the depiction of a methane flame propagating from its upper propagation limit to its stable height. The fuel velocity for this case was 35.6 m/s and there was no co-flow present. The Reynold's number for this case was calculated to be 8242. These particular conditions caused the flame to be lifted from the burner when it reached its final steady-state position. The lift-off height at steady-state was 7.62 cm downstream from the nozzle. The upper propagation limit for this case was 23.7 cm (again, this is the axial position above which (father downstream) a locally ignited region can not counter-propagate against the incoming flow and the local ignition kernel goes out/blows off – ignition attempted closer to the nozzle than 23.7 cm permits the reaction zone to propagate upstream).

At 0 ms, a), the flame is unable to sustain itself and the ignition source is required to keep the flame burning locally. At this point if the ignition source were removed, reaction will cease. In Fig 3 c), the flame begins to propagate without aid from the igniter. One can see the horizontal object akin to a pencil above the ruler (this is the igniter), and easily see when the flame moves away from the igniter. Also seen in Fig 3 c) is a hole at the centerline surrounded by reacting fluid at the leading edge – a structure related to those reported by Lee et al. [17, 18] for laminar jets. This structure is visible in some of the remaining photos (e, f, g) however, it is not as clear, and generally is not expected to be as discernable with turbulence and large-scale structures impacting the leading edge of the reaction zone. In addition an axially-oriented diffusion flame structure appears immediately as the reaction zone begins to propagate upstream away from the igniter (this is seen in the images) and remains the entire time. The total time for the flame to fully propagate from the upper propagation limit to its stable height of 7.62 cm is approximately 800 ms.

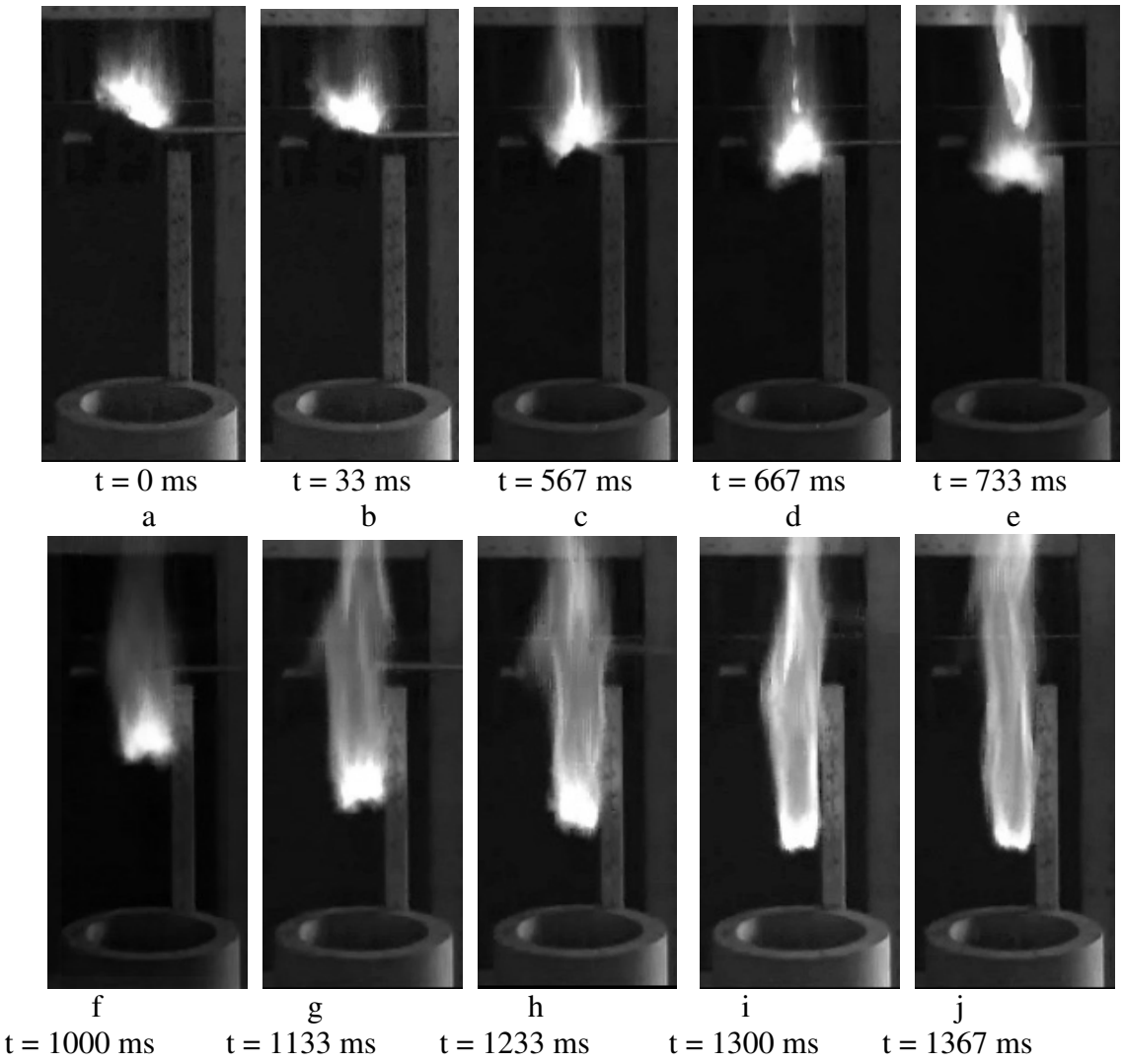

Figure 3: Propagation of methane flame from upper propagation limit (23.7 cm) to stable height (7.62 cm).

The following series of photos, figure 4, is the propagation of a flame whose fuel velocity is 35 m/s with a co-flow velocity of 0.36 m/s. These conditions correspond to a Reynold's number of 8085. For this case the upper propagation limit is 18.4 cm above the burner, and the stable height is 13.97 cm above the burner.

At time 0, Fig 4 a), the flame is not able to propagate upstream and the ignition source is required in order to keep the flame burning. However, in this case with 0.36 m/s co-flow (as compared to 0 m/s co-flow in Figure 3 a)), the structure of the flame resembles

that of the triple flame structure shown by Lee et al. [17, 18]. The appearance of the diffusion flame is also noted in b) as the propagation begins and remains the whole time. After 133 ms, b), the flame begins to propagate upstream. At this time the "triple flame" structure is not witnessed. However, it is visible in d), to some degree, 300 ms after the initial image. The total time for the flame to fully propagate from its upper propagation limit (18.4 cm) to its stable height (13.97 cm) is approximately 534 ms.

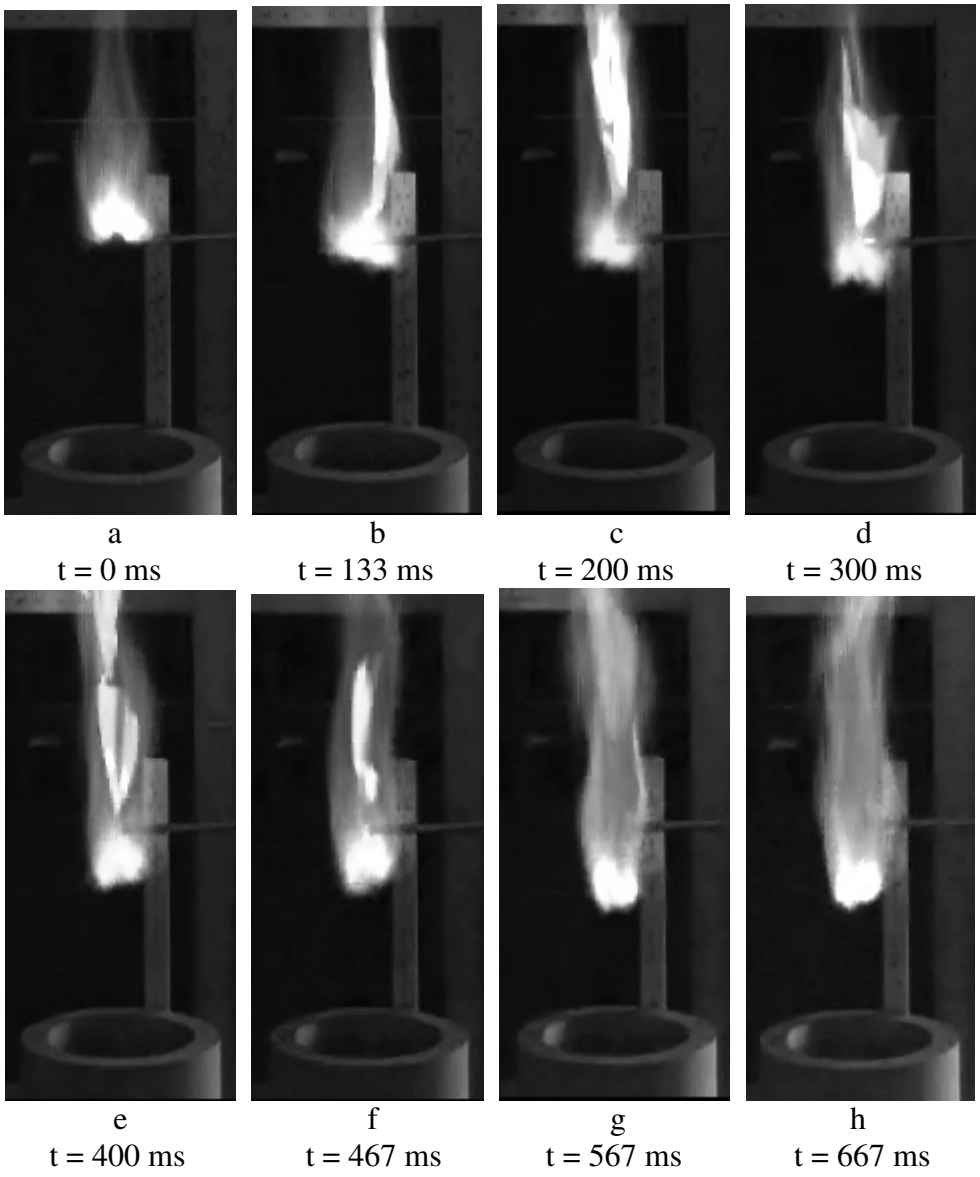

Figure 4: Propagation of methane flame from upper propagation limit (18.4 cm) to stable height (13.97 cm).

Figure 5 depicts the propagation of a methane flame from the upper propagation limit to the stable height. For this case, the fuel velocity is 13.55 m/s and the co-flow velocity is 0.49 m/s. The Reynold's number for this case is 3139. The upper propagation limit is 21 cm above the burner and the stable height is 7.62 cm above the burner.

At time 0, a), the flame is unable to sustain itself and propagate upstream as in the previous figures. However, the diffusion flame is apparent in a). Propagation upstream begins by b), after 100 ms. With the higher co-flow velocity, the hole in the center of the reaction zone is not apparent at the onset, as in the lower co-flow cases; it becomes more apparent after 533 ms as seen in figure 5 f). The general trend is witnessed in other data runs for the various co-flows. The total time taken for the flame to fully propagate to its stable height of 7.62 cm is approximately 600 ms.

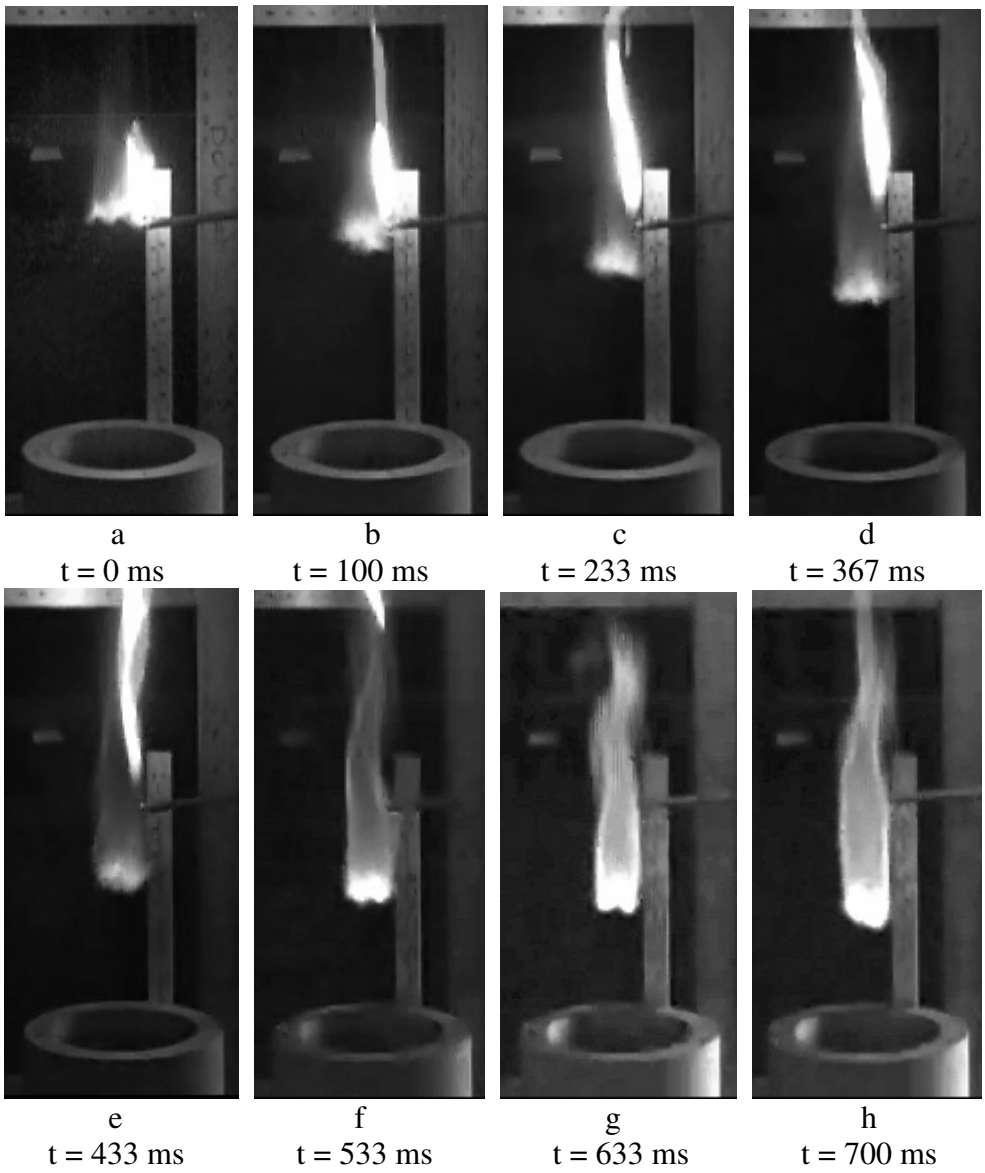

Figure 5: Propagation of methane flame from upper propagation limit (21 cm) to its stable height (7.62 cm).

The next several figures show the remaining base cases. The conditions present for each case is listed before the figure.

Figure 6 has the following conditions: fuel velocity - 42.4 m/s, co-flow velocity – 0 m/s, Reynold's number – 9823, upper propagation limit – 21.6 cm, and stable height – 10.16 cm.

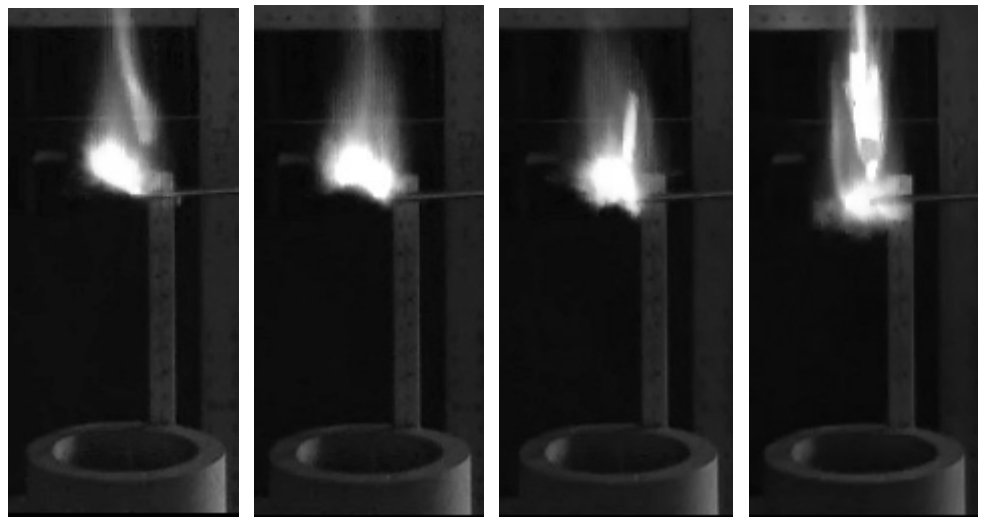

a t = 0 ms | b t = 33 ms | c t = 167 ms | d t = 333 ms

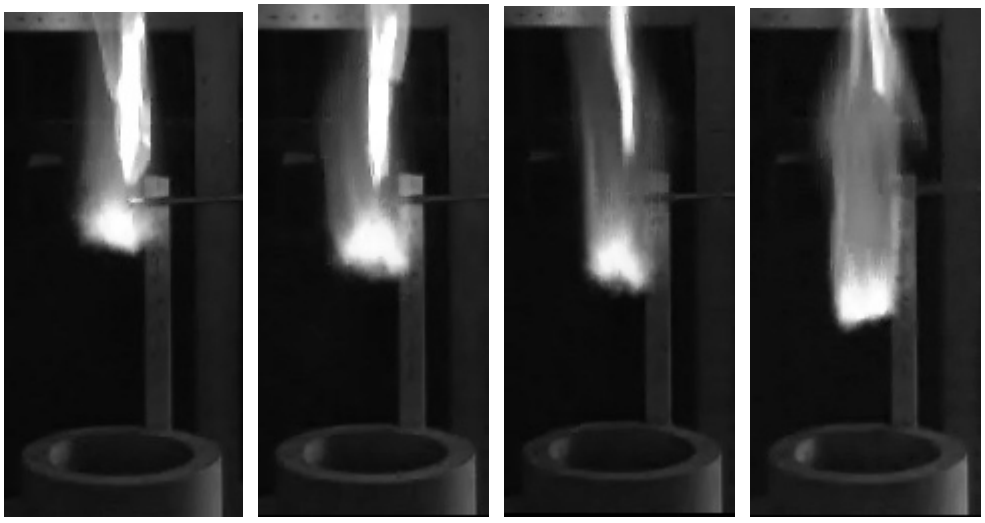

e t = 533 ms | f t = 600 ms | g t = 667 ms | h t = 800 ms

Figure 6: Propagation of methane flame from upper propagation limit (21.6 cm) to stable height (10.16 cm).

Figure 7 has the following conditions: fuel velocity – 47.3 m/s, co-flow velocity – 0 m/s, Reynold's number – 10971, upper propagation limit – 17.5 cm, and stable height – 13.97 cm.

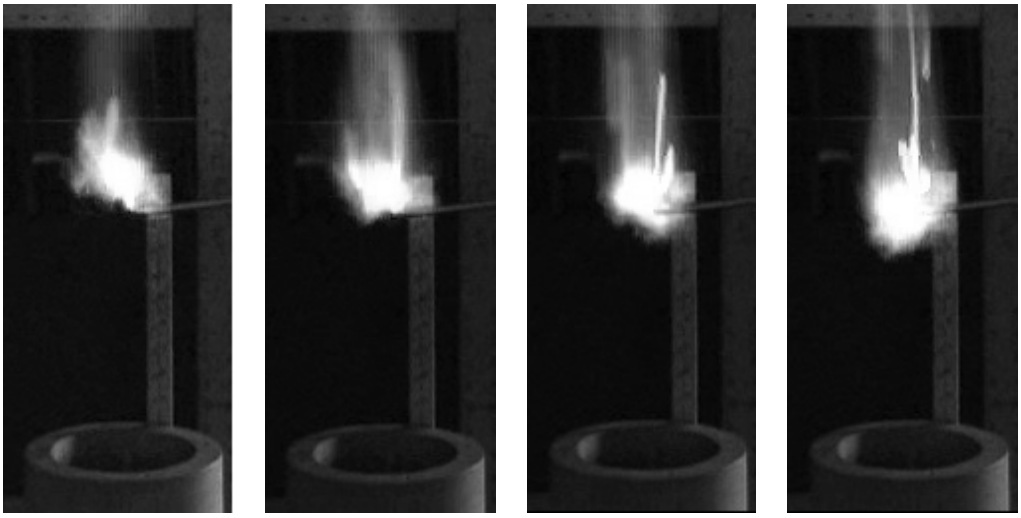

a
t = 0 ms

b
t = 67 ms

c
t = 100 ms

d
t = 133 ms

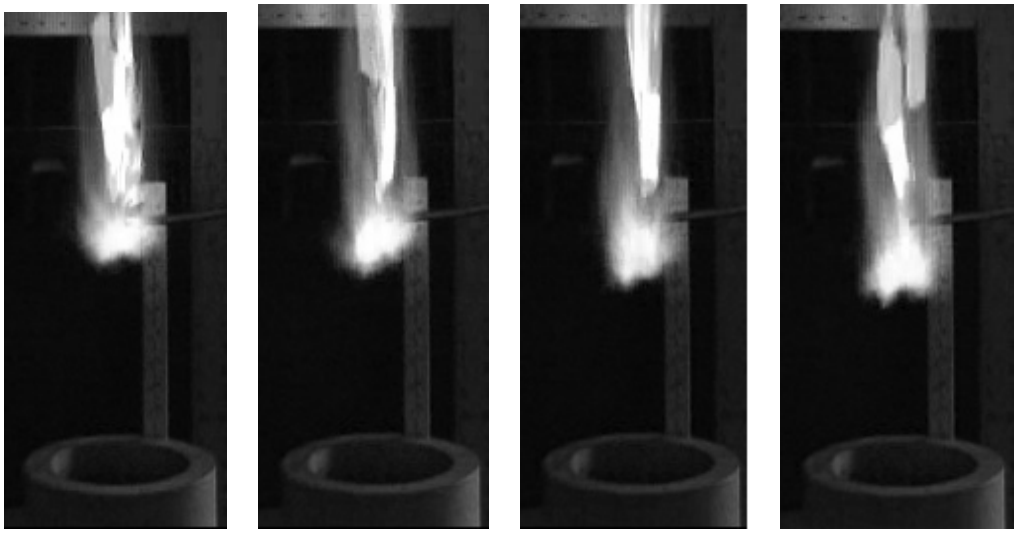

e
t = 200 ms

f
t = 267 ms

g
t = 300 ms

h
t = 333 ms

Figure 7: Propagation of methane flame from upper propagation limit (17.5 cm) to stable height (13.97 cm).

Figure 8 has the following conditions: fuel velocity – 22.64 m/s, co-flow velocity – 0.36 m/s, Reynold's number – 5247, upper propagation limit – 21 cm, and stable height – 7.62 cm.

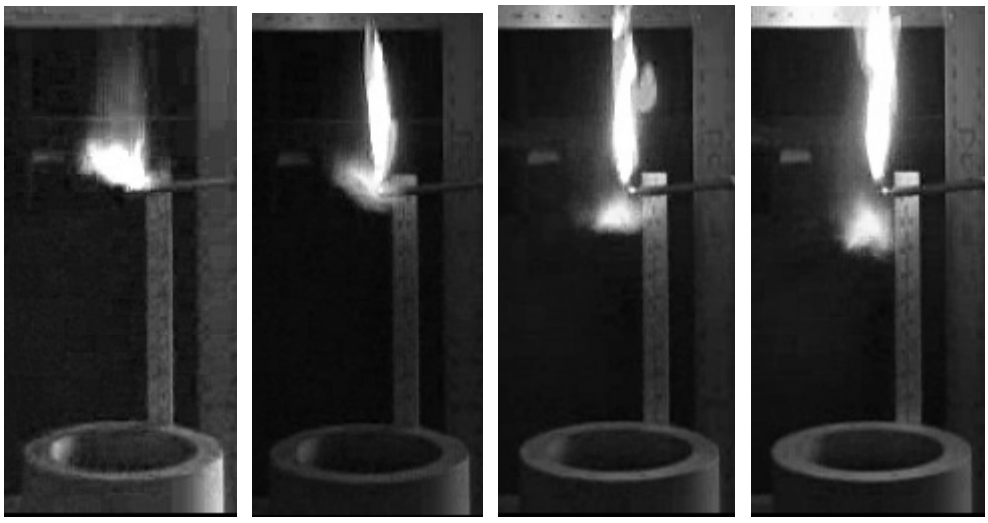

a
t = 0 ms

b
t = 67 ms

c
t = 233 ms

d
t = 333 ms

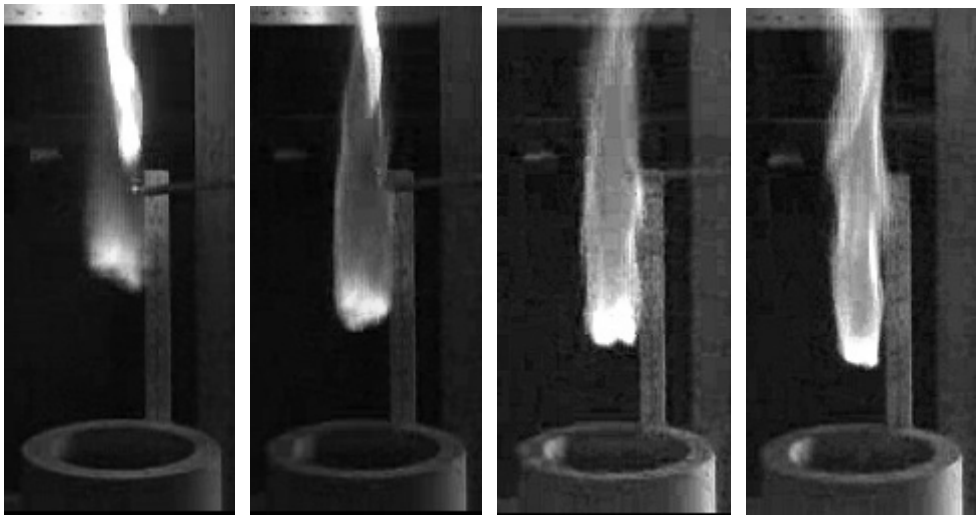

e
t = 400 ms

f
t = 533 ms

g
t = 600 ms

h
t = 733 ms

Figure 8: Propagation of methane flame from upper propagation limit (21 cm) to stable height (7.62 cm).

Figure 9 has the following conditions: fuel velocity – 29.6 m/s, co-flow velocity – 0.36 m/s, Reynold's number – 6857, upper propagation limit – 20 cm, and stable height – 10.16 cm.

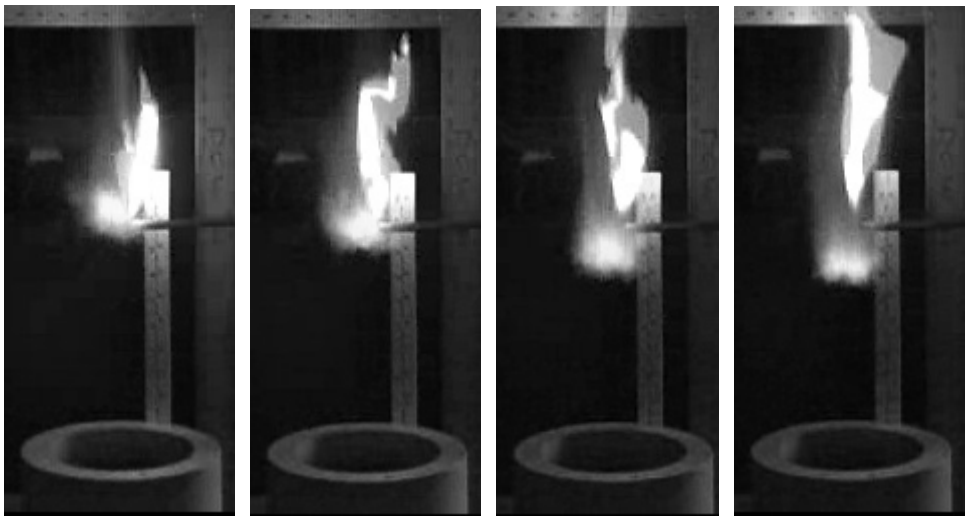

a
t = 0 ms

b
t = 33 ms

c
t = 100 ms

d
t = 167 ms

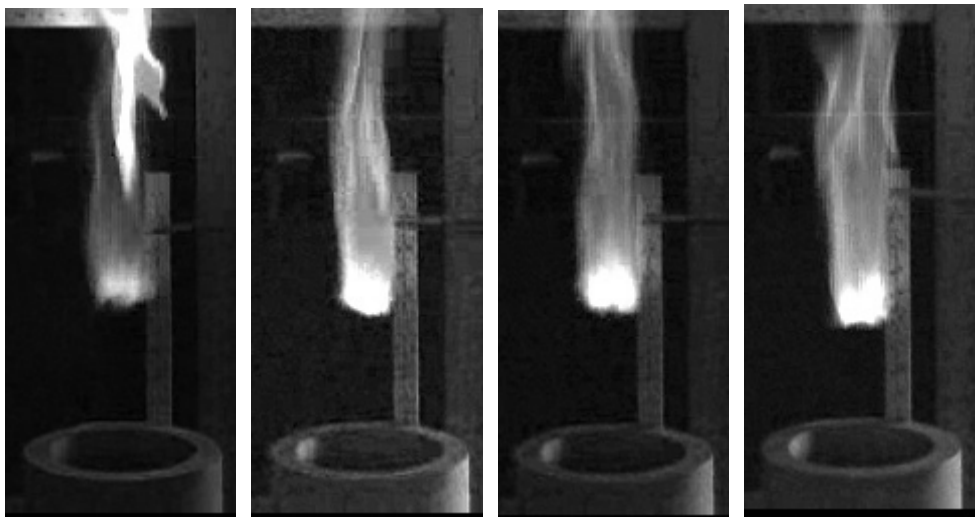

e
t = 300 ms

f
t = 500 ms

g
t = 567 ms

h
t = 733 ms

Figure 9: Propagation of methane flame from upper propagation limit (20 cm) to stable height (10.16 cm).

Figure 10 has the following conditions: fuel velocity – 22 m/s, co-flow velocity – 0.49 m/s, Reynold's number – 5106, upper propagation limit – 19 cm, and stable height – 10.16 cm.

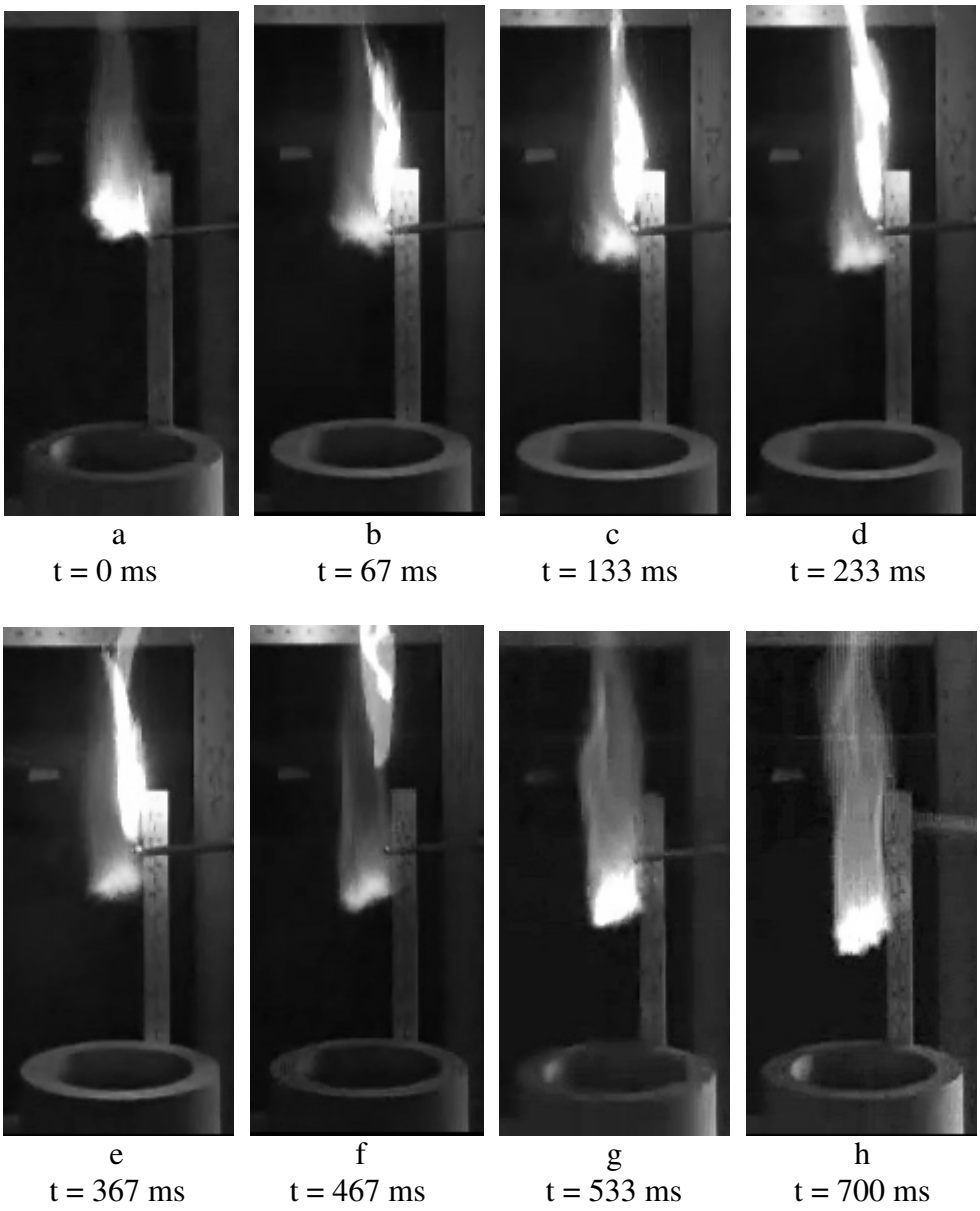

Figure 10: Propagation of methane flame from upper propagation limit (19 cm) to stable height (10.16 cm).

Figure 11 has the following conditions: fuel velocity – 26.4 m/s, co-flow velocity – 0.49 m/s, Reynold's number – 6106, upper propagation limit – 17 cm, and stable height – 13.97 cm.

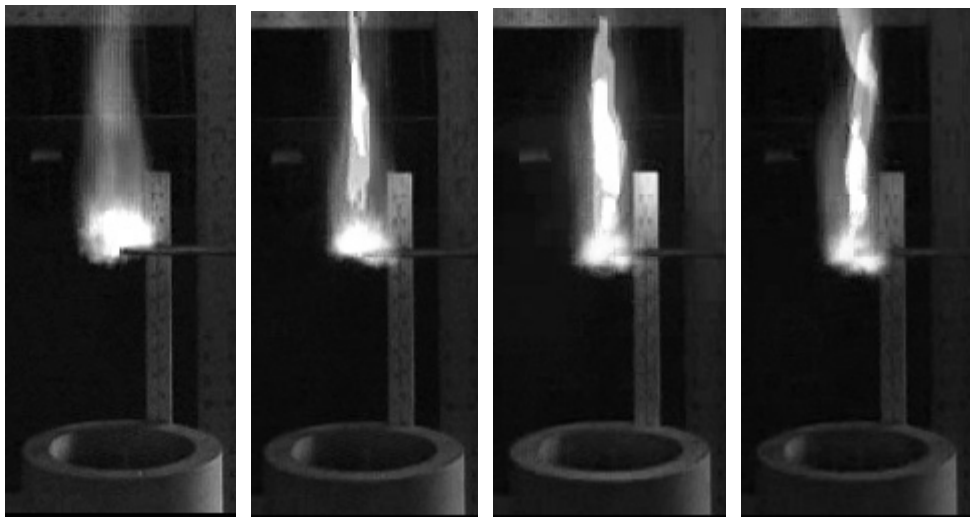

a t = 0 ms | b t = 133 ms | c t = 200 ms | d t = 267 ms

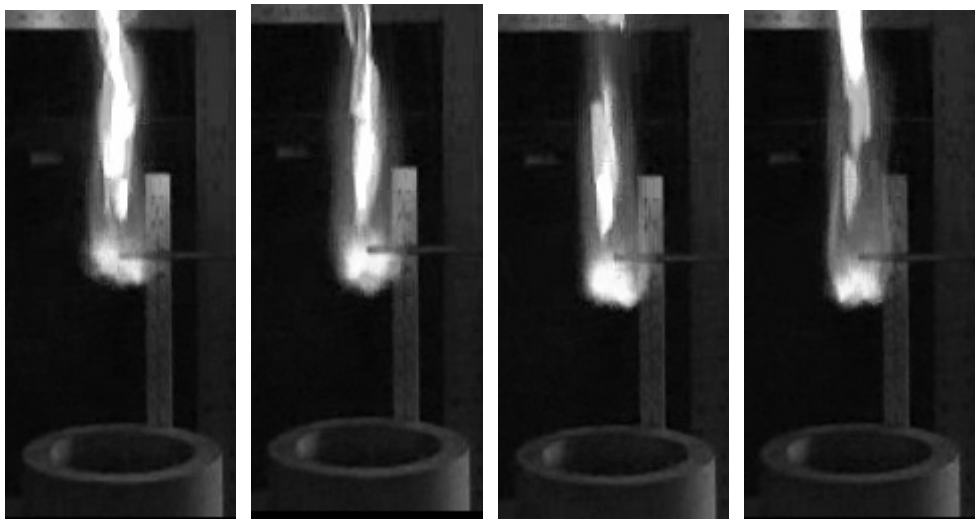

e t = 367 ms | f t = 433 ms | g t = 500 ms | h t = 600 ms

Figure 11: Propagation of methane flame from upper propagation limit (17 cm) to stable height (13.97 cm).

2.3 Upper Propagation Limit Results for Outlier Cases

The following series of photos, figure 12, shows the first outlier case at very low jet velocity. It is an outlier case because it falls outside the three co-flow, three jet velocity cases that were selected for this study in this case the low Reynold's number end. The fuel velocity for this case is 5.09 m/s and there was not any co-flow. These conditions correspond

to a Reynold's number of 1180 which produces an attached flame at steady-state rather than a lifted flame. The upper propagation limit for this case is 26 cm downstream from the burner.

At time 0, the flame cannot propagate upstream and the ignition source is required in order to keep the flame burning locally. If the ignition source is removed, the flame will completely blow-out and off. After 167 ms, c), the flame begins to propagate on its own. The trailing diffusion flame is most evident first in d) and remains visible the remainder of the time. In this case, the triple flame structure is not witnessed as it is in the other cases presented previously. However, it is slightly visible in f) and g). The total time for the flame to fully propagate from its upper propagation limit (26 cm) to its stable height (attached to burner) is approximately 866 ms.

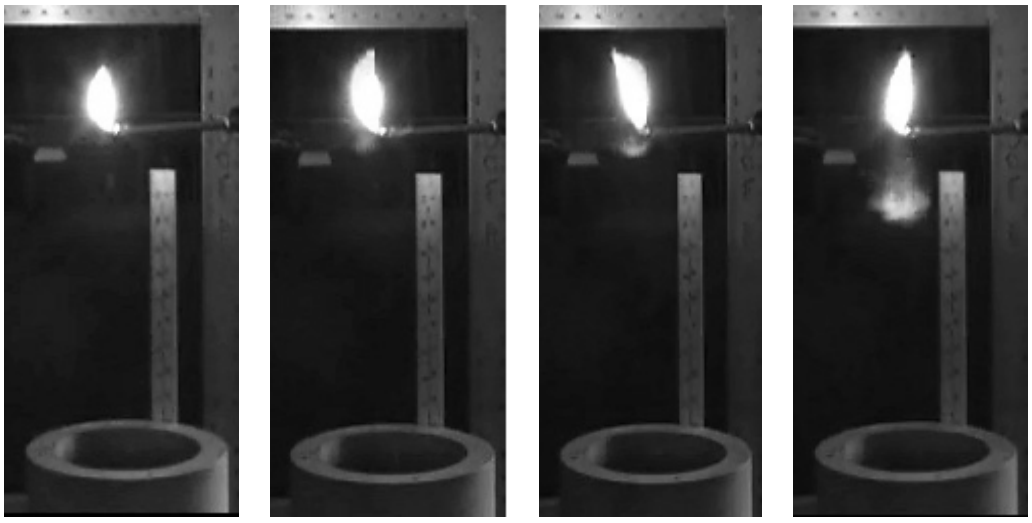

a
t = 0 ms

b
t = 100 ms

c
t = 167 ms

d
t = 300 ms

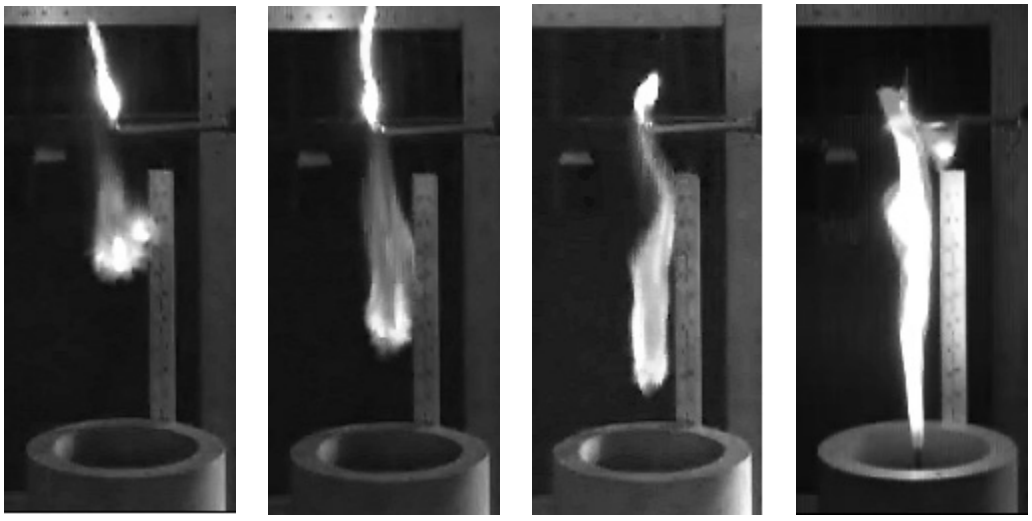

e
t = 400 ms

f
t = 500 ms

g
t = 567 ms

h
t = 1033 ms

Figure 12: Propagation of methane flame from upper propagation limit (26 cm) to stable height (attached).

Figure 13 shows the other outlier case. This is an outlier case because it also falls outside the three co-flow, three jet velocity cases probed for this study, in this case to the high Reynold's number end. The fuel velocity for this case is 49.6 m/s and there was no co-flow present. These conditions correspond to a Reynold's number of 11493 which produces

a flame that is lifted 15.24 cm above the burner. The upper propagation limit for this case is 16.5 cm downstream from the burner.

At time 0, the flame cannot propagate upstream and the ignition source is required in order to keep the flame burning locally. After 267 ms, e), the flame begins to propagate on its own. The trailing diffusion flame is evident from a) and remains visible the remainder of the time. In this case, the triple flame structure is not very pronounced at all. However, it is slightly visible in f), g), and h). The total time for the flame to fully propagate from its upper propagation limit (16.5 cm) to its stable height (15.24 cm) is approximately 200 ms.

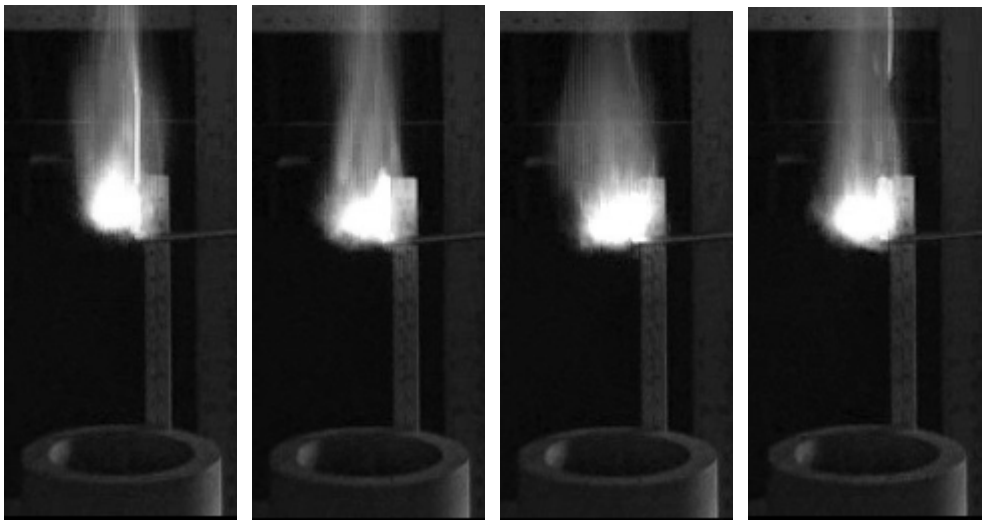

a t = 0 ms | b t = 67 ms | c t = 133 ms | d t = 200 ms

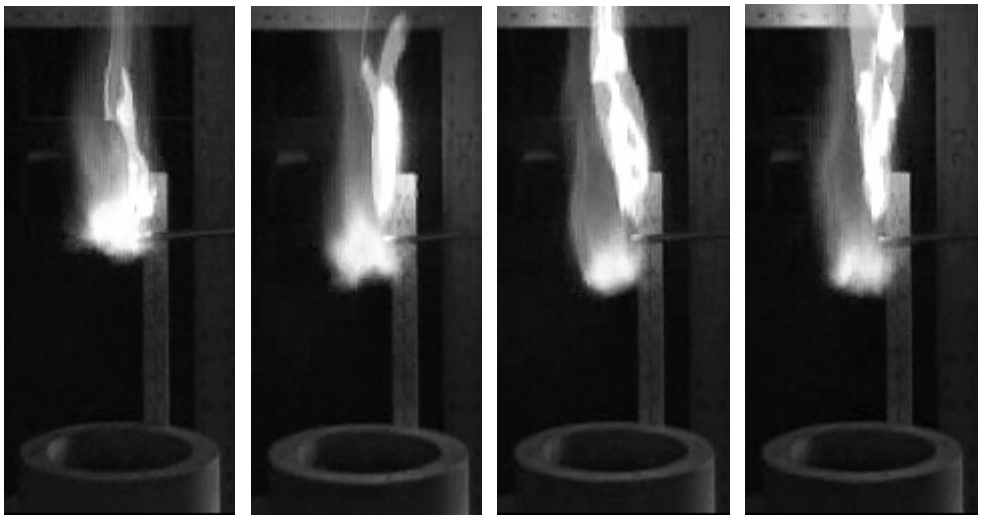

e t = 267 ms | f t = 333 ms | g t = 400 ms | h t = 467 ms

Figure 13: Propagation of methane flame from upper propagation limit (16.5 cm) to stable height (15.24 cm).

The following figure, figure 14, shows a side-by-side comparison of the propagation of the two outlier cases. The first series of photos, a), shows the propagation of an attached flame. The fuel velocity for this case is 5.09 m/s. The upper propagation limit for this case was determined to be 26 cm. The second series of photos, b), shows the propagation of a flame with a stable height of 15.24 cm above the burner. The fuel velocity for this case is

49.60 m/s. For both a), and b), there was no co-flow present. This comparison shows clearly for these cases how the upper propagation limit changes with stable position. As the stable position of the eventually steady-state flame increases in axially distance, the upper propagation limit decreases in axial distance. The upper propagation limit for a) is 26 cm and for b) is 16.5 cm; the steady-state stabilization position for a) is 0 cm (the nozzle exit) and for b) is 13.5 cm.

a.)

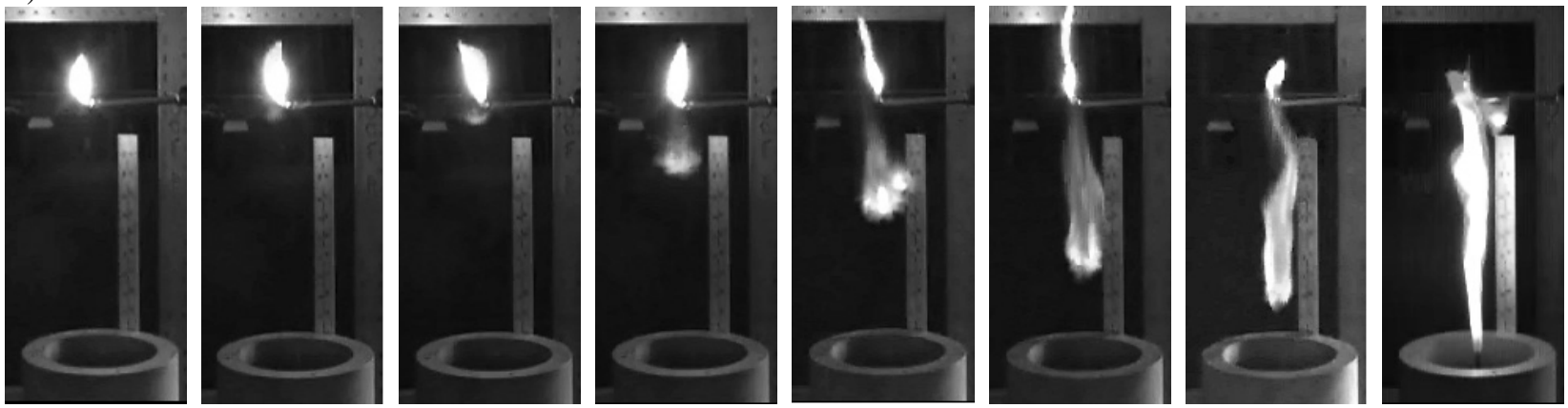

t = 0 ms t = 100 ms t = 167 ms t = 300 ms t = 400 ms t = 500 ms t = 567 ms t = 1033 ms

b.)

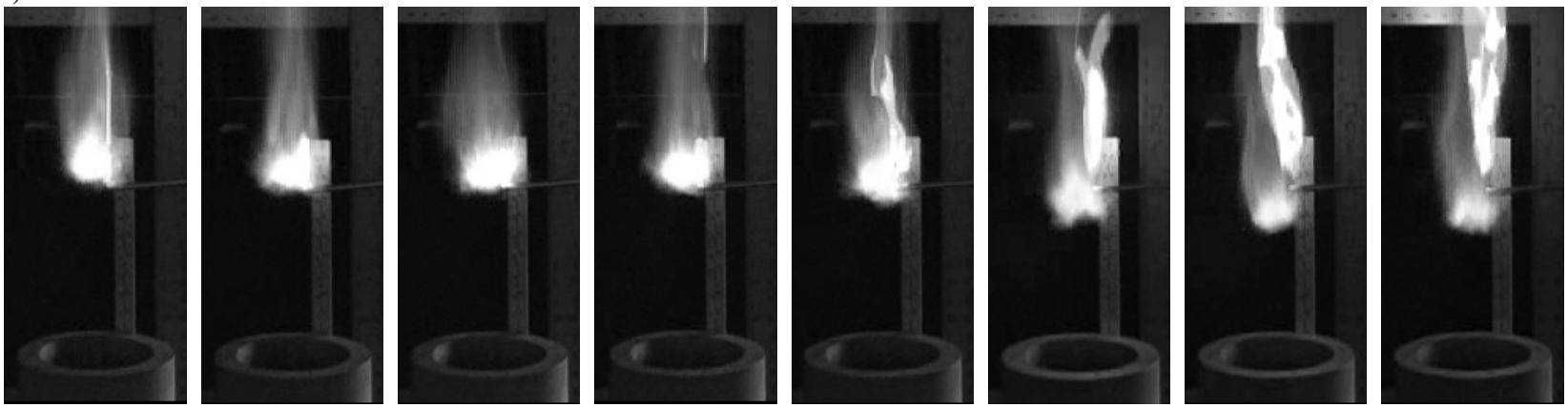

t = 0 ms t = 67 ms t = 133 ms t = 200 ms t = 267 ms t = 333 ms t = 400 ms t = 467 ms

Figure 14: Side-by-Side Comparison of Methane Flame

The data for all eleven cases is summarized in table 1. In the table, the fuel velocity and co-flow velocity for each case are listed. Also given in the table is the corresponding Reynolds number for each case and the upper propagation limit. The Reynolds number was calculated using the fuel velocity, and the density and viscosity of methane. The lifted height is the height that the lifted (or burner stabilized) flame settles to after upstream propagation.

Table 1: Experimental data for all eleven cases

Case Number	Fuel Flow Rate (slpm)	Fuel Velocity (m/s)	Co-Flow (m/s)	Lifted Height (cm)	Reynolds Number	Upper Propagation Limit (cm)	Us (m/s)
1	2.94	5.09	0	0	1180.26	26	0.28
2	20.53	35.56	0	7.62	8241.73	23.7	1.96
3	24.47	42.39	0	10.16	9823.43	21.6	2.33
4	27.33	47.34	0	13.97	10971.57	20	2.60
5	13.07	22.64	0.36	7.62	5246.93	21	1.59
6	17.08	29.59	0.36	10.16	6856.73	20	1.97
7	20.14	34.89	0.36	13.97	8085.16	18.4	2.26
8	7.82	13.55	0.49	7.62	3139.32	21	1.21
9	12.72	22.03	0.49	10.16	5106.42	19	1.67
10	15.21	26.35	0.49	13.97	6106.02	17	1.91
11	28.63	49.60	0	15.24	11493.46	18.5	2.73

The upper propagation limit has an interesting relationship with the steady-state height. As can be seen in figure 8, the upper propagation limit decreases as the steady-state height of the flame increases. The two curves become closer and closer together. The upper propagation limit and stable height are both plotted on the same graph verses the fuel velocity for each co-flow velocity case. This reinforces, physically, as a trend the behavior rendered in figure 7 that with a fixed ignition source, the upper propagation limit is inversely proportional to steady-state stabilization position: large UPL, figure 7 a), correlates with small steady-state stabilization position and small UPL, figure 7 b), corresponds to a relatively large steady-state stabilization position. If the stable height curve and the upper

propagation limit curve are extended in figure 8, they will eventually intersect with one another. At the point where these two curves cross, achieving a stable flame is not possible away from the ignition source. The flame completely blows-off and out when the ignition source is removed.

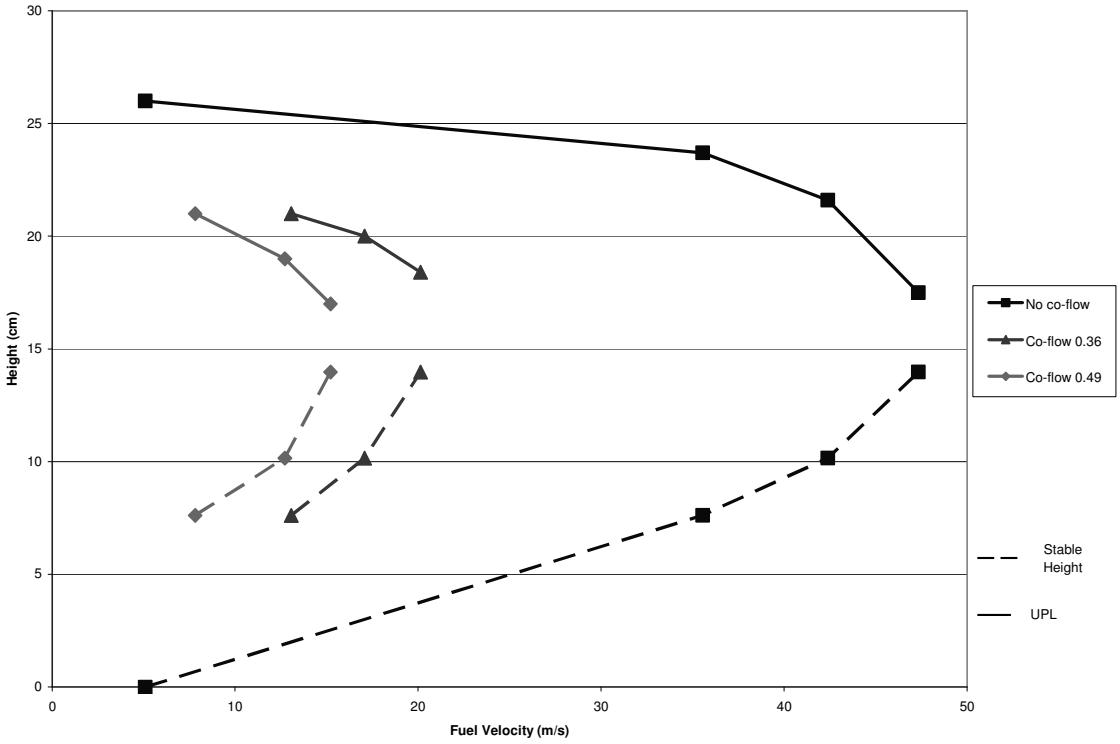

Figure 15: The upper propagation limit and stable height vs. fuel velocity.

2.4 Determinnation of the Stoichiometric Contour Velocity

The last column of table 1 is the calculated velocity on the flame surface corresponding to the stoichiometric contour, U_S. This was calculated using the following relation found in Han and Mungal [19]:

$$U_S = Z_S U_0 + (1 - Z_S) U_{CF}$$

where Z_S is the stoichiometric mixture fraction, U_0 is the nozzle exit velocity, and U_{CF} is the co-flow velocity. The assumptions made in order to apply this relation are that the jet and

co-flow velocities exhibit top-hat exit profiles, the Schmidt number is one, and there is uniform pressure [20]. For these cases $Z_S = 0.055$.

Han and Mungal [19] argue that the stoichiometric contour velocity is a good measure of the mixing between the jet and the surrounding fluid. If U_S remains unchanged for different co-flow velocities, this would imply that the flame is premixed.

After examining U_S for the above cases, it was determined that additional experiments should be conducted in order to come to a conclusion about the stoichiometric contour velocity and the laminar burning velocity. The summary of the additional experiments is given in table 2. From these experiments, the breaking point for when the flame can propagate back to the burner is determined. The reason for doing this was to determine the greatest U_S for which the flame could propagate back to the burner. This U_S can then be compared to the laminar burning velocity to determine if there exists a connection between the two and the ability of the flame to propagate, and also U_S can be compared among the various co-flow velocity cases.

Table 2: Stoichiometric contour velocity for the breaking point of liftoff.

Bob Height (mm)	Fuel Flow Rate (slpm)	Fuel Velocity (m/s)	Co-Flow (m/s)	Us (m/s)
23	7.14	12.37	0	0.68
10	2.94	5.09	0.36	0.62
9	2.64	4.57	0.49	0.71
5	1.42	2.46	0.61	0.71
7	2.03	3.52	0.73	0.88

It is found that the maximum stoichiometric contour velocity remains nearly the same regardless of the co-flow velocity. This observation, in addition to the appearance of the triple flame structure, leads to further support the premixed flame propagation in permitting

these flames to not only propagate from the upper propagation limit position, but also to propagate back to the burner.

3. Summary

3.1. Conclusions

The images given in figures 3 through 13 show the propagation of a methane flame. From these images, the upper propagation limit was determined. Increasing the jet Reynold's number, for constant co-flow velocity, has an inverse effect on the upper propagation limit. As the co-flow velocity is increased, also seen is an inverse effect on the upper propagation limit. One possible explanation is that this is, in part, due to enhanced mixing of fuel and air with co-flow. The added co-flow allows for better mixing to occur closer to the burner. When this happens, the fuel and air downstream will be well-mixed but with further entrained air, generally too lean to support propagation for the given axial velocities. This idea is consistent with the fact that it is indeed the premixed flame which supports flame propagation (Lifted Flame Stabilization) as opposed to the extinction of the diffusion flame at the leading edge [21].

The last column of table 1 gives the stoichiometric contour velocity, U_S. The relation used to calculate this velocity accounted for the fuel velocity as well as the co-flow velocity. The laminar burning velocity (S_L) for methane is approximately 43 cm/s. In each case that produced a U_S less than S_L, the flame was observed to burn all the way upstream to the burner, never stabilizing as a steady-state lifted flame. This can be seen in figure 12 which corresponds to case 1 in table 1. For this case, U_S is 28 cm/s and the flame is observed to burn all the way back to stabilize at the burner. However, when U_S was determined to be greater than S_L, the flame was not able to burn back to the burner and stabilized downstream

in the mixing region of jet fluid and co-flow air. This can be seen in figure 5 which corresponds to case 8 in table 1. For this case, the flame is observed to only propagate to a steady-state position of 7.62 cm above the burner. The U_S for this case was determined to be 121 cm/s which is greater than S_L. However, when the additional tests were conducted in order to determine the maximum U_S for which the flame would still propagate back to the burner, it was discovered that the maximum is in excess of S_L. In other words, the reaction zone was able to propagate upstream into regions in excess of the planer laminar burning velocity. However, S_L has direct correspondence only to one-dimensional laminar flame-front cases. All the above cases are turbulent. For turbulent cases it has been argued that the burning velocity can be as large as three times the S_L for flame stabilization [16], similar magnitudes were argued by Watson et al. [22]. In all the tests that were performed, the greatest U_S found was 88 cm/s, approximately $2S_L$ which falls within the bounds of the previous metrics. It is surprising that this simple relation weighting the co-flow velocity and jet fluid velocity with stoichiometric contour could produce agreement for all the cases probed. It is also interesting to note that as U_S increases, the stable axial position where the flame settles to also increases.

3.2. Future Work

The results of this study show how the Reynolds number and the co-flow velocity affect the upper propagation limit. This data supports the idea that the premixed propagation is what dictates flame stabilization rather than the extinction of the diffusion flame [21], though some experiments are still investigating scalar dissipation as the controlling parameter [23] and hybrid approaches may still be feasible [15]. The next part of this study will consist of the same type of experiments as previously described, however, instead of

keeping the lifted height constant, the fuel velocity will be held constant for varying co-flow velocities. This will allow for a closer examination of the relationship between U_S and the upper propagation limit. Experiments including the different morphologies of the leading-edge flames at different co-flow velocities and liftoff heights are also in progress to assess the effects of heat release on streamline divergence and stabilization location.

4. References

[1] Maurey, C., Cessou, A., Lecodier, B. and Stepowski, D., 2000, "Statistical Flow Dynamics Properties Conditioned on the Oscillating Stabilization Location of Turbulent Lifted Flame", Twenty-Eighth Symposium (International) on Combustion / The Combustion Institute, 2000, pp. 545-551.

[2] Lyons, K. M. and Watson, K. A., 2001, "Visualizing Diffusion Flame Formation in the Wake of Partially Premixed Combustion", ASME Journal of Energy Resources Technology, 123 (3): 221-227.

[3] Wohl, K., Kapp, N. M., and Gazley, C., 1949, "The Stability of Open Flames", Third Symposium on Combustion and Flame, and Explosion Phenomena, The Williams and Wilkins Company, pp. 3-21.

[4] Vanquickenborne, L. and van Tiggelen, A., "The stabilization mechanism of lifted diffusion flames", Combustion and Flame, 10, pp. 59-69, 1966.

[5] Eickhoff, H., Lenze, B. and Leuckel, W., "Experimental Investigation on the Stabilization Mechanism of Jet Diffusion Flames", Twentieth Symposium (International) on Combustion / The Combustion Institute, 1984, pp. 311-318.

[6] Kalghatgi, G. T. "Lift-off Heights and Visible Lengths of Vertical Turbulent Jet Diffusion Flames in Still Air", Combustion Science and Technology, 1984, Vol. 41, pp. 17-29.

[7] Brown, C. D., Watson, K. A., and Lyons, K. M., 1999, "Studies on Lifted Jet Flames in Coflow: The Stabilization Mechanism in the Near- and Far-Fields", Flow Turbulence and Combustion, 62, pp. 249-273.

[8] Broadwell, J. E., Dahm, W. J. A., and Mungal, M. G., Twentieth Symposium (International) on Combustion / The Combustion Institute, 1984, pp. 303-310.

[9] Clemens, N. T. and Paul, P. H., "Effects of Heat Release on the Near Field Flow Structure of Hydrogen Jet Diffusion Flames", Combustion and Flame, 102, pp. 271-284, 1995.

[10] Yamashita, H., Shimada, M., and Takeno, T., "A Numerical Study on Flame Stability at Transition Point of Jet Diffusion Flames", Twenty-Sixth Symposium (International) on Combustion / The Combustion Institute, 1996, pp. 27-34.

[11] Peters, N. and Williams, F. A., "Lift-off Characteristics of Turbulent Jet Diffusion Flames", AIAA Journal, **21** (3), pp. 423-429, 1983.

[12] Phillips, H., "Flame in a Buoyant Methane Layer", Tenth Symposium (International) on Combustion / The Combustion Institute, 1965, pp. 1277-1283.

[13] Liñán, A., "Ignition and Flame Spread in Laminar Mixing Layers", Combustion in High-Speed Flows, Kluwer Academic, Dordrecht, 1994, pp. 461-476.

[14] Veyante, D., Duclos, J. M., and Piana, J., "Experimental Analysis of Flamelet Models for Premixed Turbulent Combustion", Twenty-Fifth Symposium (International) on Combustion / The Combustion Institute, 1994b, pp. 1249-1256.

[15] Müller, C. M., Breitbach, H., and Peters, N., "Partially Premixed Turbulent Flame Propagation in Jet Flames", Twenty-Fifth Symposium (International) on Combustion / The Combustion Institute, 1994, pp. 1099-1106.

[16] Muñiz, L., and Mungal, M. G., "Instantaneous Flame-Stabilization Velocities in Lifted-Jet Diffusion Flames", Combustion and Flame, 1997, Vol. 111, pp. 16-31.

[17] Lee, B. J., Kim, J. S. and Chung, S. H., "Effect of Dilution on the Liftoff of Non-Premixed Jet Flames," Twenty-Fifth Symposium (International) on Combustion / The Combustion Institute, 1994, pp. 1175-1181.

[18] Lee, B.J. and Chung, S.H., "Stabilization of Lifted Tribrachial Flames in a Laminar Nonpremixed Jet", Combustion and Flame, 109, pp. 163-172.

[19] Han, D. and Mungal, M. G., "Observations on the Transition from Flame Liftoff to Flame Blowout", Twenty-Eighth Symposium (International) on Combustion / The Combustion Institute, 2000, pp. 537-543.

[20] Kuo, K. K., Principles of Combustion, 2nd Edition, 2005.

[21] Peters, N., Turbulent Combustion, 1st Edition, 2000.

[22] Watson, K. A., Lyons, K. M., Donbar, J. M., and Carter, C. D., "Simultaneous Two-Shot CH-PLIF and Particle Image Velocimetry Measurements in Lifted CH4-Air Diffusion Flames", Twenty-Ninth Symposium (International) on Combustion / The Combustion Institute, 2002, pp. 1905-1912.

[23] Noda, S., Mori, H., Hongo, Y. and Nishioka, M., “Nonpremixed Flamelet Statistics at Flame Base of Lifted Turbulent Jet Nonpremixed Flames”, JSME International Journal, 46, pp. 75-82.